NASA TECHNICAL NOTE

NASA TN D-5149

c. 1

LOAN COPY: RE
AFWL (WLI
KIRTLAND AFB,

TECH LIBRARY KAFB, NM
0131931

NASA TN D-5149

EVALUATION OF A PILOT DESCRIBING FUNCTION METHOD APPLIED TO THE MANUAL CONTROL ANALYSIS OF A LARGE FLEXIBLE BOOSTER

by Dallas G. Denery and Brent Y. Creer

Ames Research Center
Moffett Field, Calif.

RECEIVED
15 APR 1969
Technical Library
AFWL (WLIL-2)
Laboratory

NATIONAL AERONAUTICS AND SPACE ADMINISTRATION • WASHINGTON, D. C. • APRIL 1969

TECH LIBRARY KAFB, NM
0131931

EVALUATION OF A PILOT DESCRIBING FUNCTION METHOD APPLIED TO THE MANUAL CONTROL ANALYSIS OF A LARGE FLEXIBLE BOOSTER

By Dallas G. Denery and Brent Y. Creer

Ames Research Center
Moffett Field, Calif.

NATIONAL AERONAUTICS AND SPACE ADMINISTRATION

For sale by the Clearinghouse for Federal Scientific and Technical Information
Springfield, Virginia 22151 – CFSTI price $3.00

EVALUATION OF A PILOT DESCRIBING FUNCTION METHOD APPLIED TO THE MANUAL CONTROL ANALYSIS OF A LARGE FLEXIBLE BOOSTER

By Dallas G. Denery and Brent Y. Creer

Ames Research Center

SUMMARY

In the pilot describing function technique of manual control analysis, the pilot is represented by a linear describing function and a statistically described "remnant." The remnant accounts for that part of the pilot output not linearly correlated with the input. The technique was pioneered in work on manual control of rigid vehicles and has resulted in a catalog of pilot describing functions and remnant data applicable to certain pilot tasks. The applicability of this technique and of the existing data to the analysis of manual control of a flexible vehicle had not been investigated. In this report, the method is evaluated for use in analyzing the pilot control of a large flexible booster.

There are two phases in the present investigation. In the first, the pilot describing function method is evaluated when applied to the analysis of pilot control of an uncompensated booster. A piloted flight simulator is used and the pilot describing function, remnant and performance opinion ratings are measured. These quantities are compared with those estimated using data obtained from essentially rigid vehicle manual control problems. In the second phase, the pilot describing function method is evaluated when used to define a compensation system for the flexible booster. Pilot opinion ratings measured for this compensation system, using a flight simulator, are compared with ratings estimated using the pilot describing function method. These ratings are also compared with those measured for a different compensation system which was based on the same criteria, but deduced by an entirely different method of analysis employing piloted flight simulators exclusively.

It is concluded that the remnant part of the pilot model assumes a greater importance in the analysis of a flexible vehicle than in the analysis of rigid body manual control because of its tendency to excite the structural modes. The pilot remnant estimated from the existing data does not appear definitive enough to use in the manual control analysis of a flexible booster. However, the pilot describing function method affords a valuable technique that can be used in conjunction with a simulator program for defining an adequate manual control system for a flexible booster.

INTRODUCTION

The NASA has conducted a general research program concerned with pilot control of the Saturn V launch vehicle. The initial phase of this study dealt with piloting problems involved in guiding the vehicle through the first stage without overloading the structure during encounters with wind disturbances. Two main problems have been attacked. The first is the feasibility of pilot control of the uncompensated booster and the second is the definition of a suitable compensation system of minimum complexity. The solution to each of these problems was sought by two methods. In the first, termed the flight simulator method, the launch vehicle and pilot task were simulated and an experimental investigation conducted. In the second, termed the pilot describing function method, the system was analyzed using pilot describing functions and servomechanism theory. The flight simulator method of analysis proceeded along conventional lines and is described in reference 1. The pilot describing function method was used by Systems Technology, Inc., under contract to the NASA (refs. 2 and 3).

Basically, the pilot describing function method can be considered as a two step process. In the first step, the pilot task is simplified to that of minimizing a single error signal and is usually referred to as a single-axis compensatory tracking task. As shown in figure 1, the pilot is represented by a describing function, Y_p, and an injected noise termed "remnant" $n_e(t)$ (ref. 4). The remnant is used to describe that part of the pilot output $c(t)$ not linearly correlated with the system input $i(t)$. With such a pilot representation, the performance of this simplified pilot-vehicle system may be analyzed using the standard techniques of servomechanism theory. The second part of the process is to use information from the single-axis compensatory analysis to predict the performance of a pilot flying the actual system in the operational task. This is a far less definitive process than the first part since it accounts for additional factors (such as complexity and workload), and relies heavily on the past experience of the analyst.

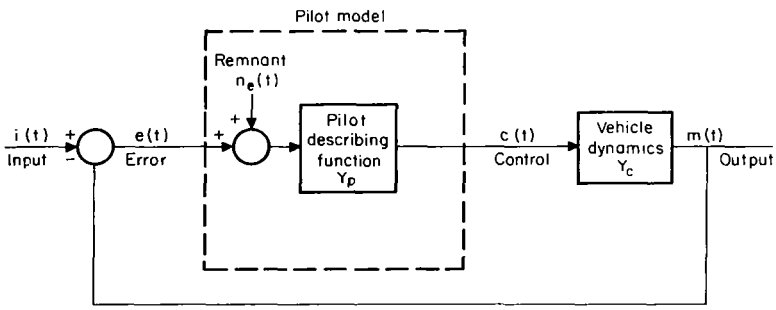

Figure 1.- General representation for manual control in a single-axis compensatory tracking task.

The pilot describing function method has been used successfully in the field of manual control analysis to support simulation efforts and to make independent preliminary analysis of certain pilot control problems (refs. 5 and 6). Generally, the structural flexibility of the vehicle has been considered negligible. In the manual control analysis of large flexible boosters, however, such effects must be included (refs. 7 and 8). The Saturn V vehicle is characterized by a high degree of structural flexibility. The application

of the existing pilot describing function data to this new class of vehicle could therefore be questioned because of the unknown influence of the structural flexibility.

The effect of pilot remnant in the analysis is of particular concern. Pilot remnant can often be neglected in the analysis of manual control of rigid vehicles. This is not true in the analysis of manual control of flexible vehicles. The pilot output that corresponds to the remnant is generally a small portion of the total pilot output. However, at high frequencies, the remnant is often the only source of excitation in an otherwise linear system. During the manual control of rigid vehicles, the high-frequency remnant is filtered by the vehicle dynamics and does not affect the system performance. During the manual control of a flexible vehicle, the high-frequency remnant excites the elastic modes whose effect is therefore amplified. In this case, the pilot remnant would have a definite effect on system performance.

The limitations of the describing function and remnant data for manual control of elastic vehicles were fully recognized at the time of the study by Systems Technology, Inc. However, it was agreed that the best available models[1] would be used by Systems Technology, Inc., to independently analyze this new type of pilot-vehicle system, and to later compare the results with the more conventional simulator program. Specific areas, such as pilot describing functions and remnant spectra, were to be investigated experimentally at Ames to validate or refine the models and parameters used in the analysis performed by Systems Technology, Inc. These data are presented in this report. The overall goals of this report are to indicate the applicability of the describing function method to the manual control of large flexible boosters and to reveal the areas needing more research.

NOTATION

$c(t)$	pilot output signal
$e(t)$	error signal
F_α, F_θ	time-varying coefficients in the equations of motion
g	earth's gravirotational acceleration, m/sec^2
$i(t)$	system input signal
j	imaginary unit, $\sqrt{-1}$
M_α, M_β	time-varying coefficients in the equations of motion
$m(t)$	system output signal

[1]This analysis was performed in 1965. Since that time, additional work on pilot modeling has been performed. (See refs. 9 and 10.)

$n_e(t)$	noise signal injected into system at pilot perception point
s	Laplace variable
V	velocity, m/sec
Y_c	vehicle transfer function
Y_p	pilot describing function
α	aerodynamic angle of attack, deg
β	engine gimbal angle, deg
γ_p, γ_a	acceleration at pilot and accelerometer locations, respectively, m/sec^2
$\Delta\theta_{AG}, \theta_{AG}, \dot{\theta}_{AG}$	deviation of attitude from nominal trajectory, attitude and attitude rate measured at attitude gyro location, deg/deg/sec
$\Delta\theta_{RG}, \theta_{RG}, \dot{\theta}_{RG}$	deviation of attitude from nominal trajectory, attitude and attitude rate measured at rate gyro location, deg/deg/sec
σ	standard deviation
$\Phi_{xy}(j\omega)$	cross power density function between signals $x(t)$ and $y(t)$ where $\frac{1}{2\pi}\int_0^\infty \lvert\Phi_{xx}(j\omega)\rvert^2 d\omega = \sigma^2$
ω	frequency, rad/sec

VEHICLE AND DISTURBANCE

The vehicle configuration and pertinent dimensional data are shown in figure 2. Fully fueled, the vehicle mass is nearly 3,000,000 kg, and the moment of inertia approximately 1×10^6 kg-m^2. The natural frequencies of the first two bending modes are 1 and 2 Hz, respectively.

Only the first stage of flight is considered. This stage follows a gravity turn trajectory for 150 seconds. Burnout occurs at an altitude of approximately 60,000 m, with a velocity of 2,350 m/sec. The maximum thrust-to-weight ratio is 4.7. The maximum dynamic pressure is 3,650 kg/m^2 and occurs 77 seconds after lift-off at an altitude near 13,000 m.

Severe structural loads are caused by winds that occur near the maximum dynamic pressure portion of the trajectory. Part of the pilot task is to reduce these wind-induced loads. A wind disturbance based on measurements taken at the Air Force Eastern Test Range, Cape Kennedy Launch Area (ref. 1), was assumed in the investigation and is described in appendix B.

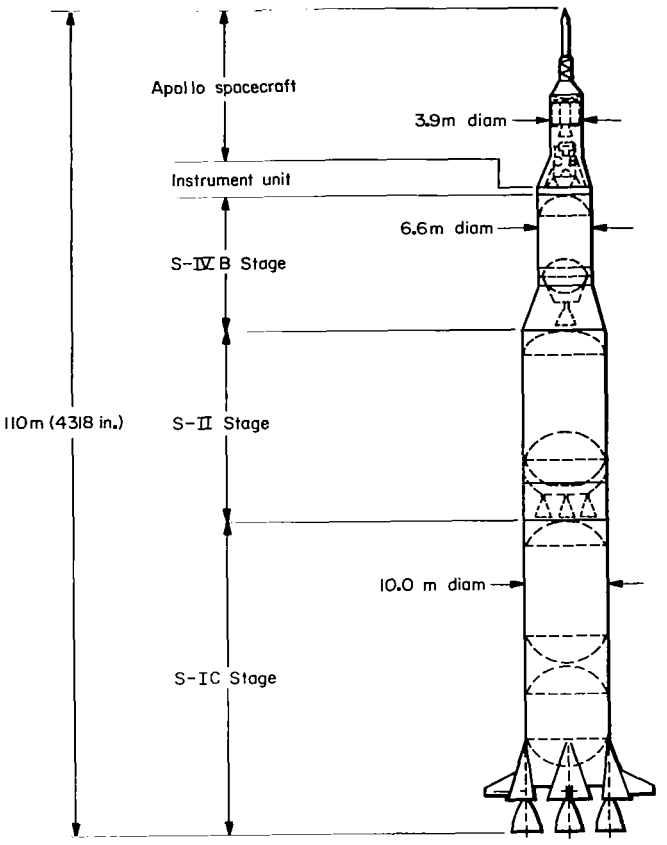

Figure 2.- Saturn V vehicle configuration.

PERFORMANCE CRITERIA

The performance measures considered are contained in reference 3. Briefly, these criteria were tracking accuracy, structural loads (bending moments), transverse accelerations at the pilot station, and pilot opinion. The structural loads are computed in the form M/Md, defined as the ratio of maximum bending moment to the design bending moment at a critical location on the vehicle. Transverse acceleration at the pilot station is measured in g's. Pilot opinion is measured using the numerical Cooper Pilot Opinion Rating Scale (ref. 11). This scale is shown in figure 3.

EVALUATION PROCEDURE

The procedure used to evaluate the pilot describing function method applied to the manual control of the uncompensated

	Adjective rating	Numerical rating	Description	Primary mission accomplished
NORMAL OPERATION	Satisfactory	1	Excellent, includes optimum	Yes
		2	Good, pleasant to fly	Yes
		3	Satisfactory, but with some mildly unpleasant characteristics	Yes
EMERGENCY OPERATION	Unsatisfactory	4	Acceptable, but with unpleasant characteristics	Yes
		5	Unacceptable for normal operation	Doubtful
		6	Acceptable for emergency condition only *	Doubtful
NO OPERATION	Unacceptable	7	Unacceptable even for emergency condition*	No
		8	Unacceptable - Dangerous	No
		9	Unacceptable - Uncontrollable	No
	Unprintable	10	"Motions possibly violent enough to prevent pilot escape"	

* Failure of stability augmenter

Figure 3.- Pilot opinion rating scale.

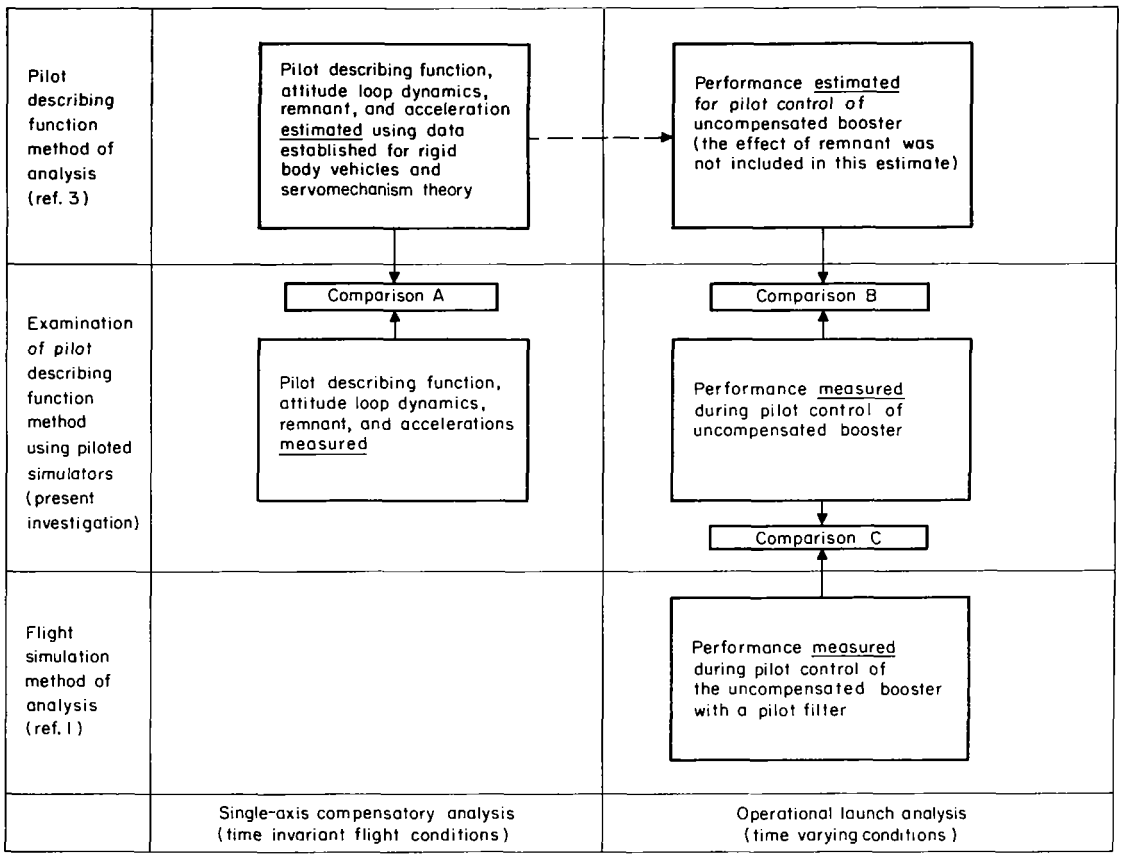

Figure 4.- Uncompensated booster.

booster is presented in figure 4. The top row illustrates the work done by Systems Technology, Inc., using the pilot describing function method (refs. 2 and 3). The middle row illustrates the work done in the present investigation, and the bottom row illustrates the work done by NASA using the flight simulator method of analysis (ref. 1). As is evident from figure 4, two different simulations were used in the present investigation. First, the uncompensated booster was simulated on a single-axis compensatory tracking task simulator. In this type of simulation, the pilot observes a single-axis error display and his task is to track a random input signal. The equations of motion were approximated by a set of time invariant equations. This simulation is further discussed in appendix B. During the piloted control of the single-axis compensatory tracking task simulator, the pilot describing function, remnant, combined pilot-vehicle frequency response, and the accelerations at the pilot station were measured. These measured quantities are compared (comparison A) with those estimated in the pilot describing function study for the single-axis compensatory analysis. Second, the uncompensated booster was simulated on a fixed-base launch vehicle simulator. Time varying equations of motion were used in this simulator, and the pilot displays were similar to those that would be used in the operational vehicle. The pilot task was to control the vehicle during a simulated launch. From this

simulation, the basic system performance was measured. Data from the launch vehicle simulation are used to make two comparisons. First, the measured data are compared (comparison B) with the performance estimated for the operational launch using the pilot describing function method (ref. 3). This comparison is made to indicate the success of the pilot describing function method in predicting the system performance for the operational task from the results obtained in the single-axis compensatory analysis phase of the pilot describing function method. Unfortunately, this step in the pilot describing function study did not include computations of the effect of pilot remnant and the comparison cannot be expected to be good. These same measured data are also compared (comparison C) with the performance data measured for the uncompensated booster manual control system studied by NASA using the flight simulator method (ref. 1). In this system, the pilot output was filtered whereas no filtering was provided in the pilot describing function analysis. This performance comparison is made to indicate the effectiveness of the pilot describing function method without remnant in the formulation of a manual control system for a flexible booster.

The procedure used to evaluate the pilot describing function method applied to the derivation of a compensated booster manual control system is illustrated in figure 5. To understand the evaluation procedure, it is essential to understand the sequence of events in the pilot describing function study. Two phases were used in this study to define a "final" compensated system. In the first phase, a preliminary system was formulated in which the remnant effects were not computed. The purpose of this system was to establish the basic stability augmentation for the system. This system was simulated in a launch vehicle simulator in the present investigation, and the results of the simulation were examined by Systems Technology, Inc. These results were used to obtain an understanding of the effect of remnant on the system performance. Using these results and published remnant data, a "final" integrated compensated booster manual control system was formulated during phase 2 of the pilot describing function study.

In the present investigation, neither the "preliminary" nor "final" compensated booster systems were simulated on the single-axis compensatory tracking task simulator. Therefore, the corresponding estimated pilot describing functions, etc., cannot be compared with simulator measured quantities. However, both preliminary and final systems were simulated on a launch vehicle simulator. The performance for these two systems is measured and is used to make three comparisons. First, the performance measured for the preliminary system (which did not include the effect of remnant) and final system is compared (comparison D). The purpose of this comparison is to indicate the effect of remnant in the formulation of a control system for a flexible booster. Second, the performance measured for the final system is compared (comparison E) with the performance estimated for that system using the pilot describing function method. The purpose of this comparison is to indicate how well the results of the single-axis compensatory analysis of the pilot describing function method can be generalized to estimate the performance in the operational task. Third, the measured performance for the final system is compared (comparison F) with the measured performance for the compensated booster that was formulated using the conventional flight simulator

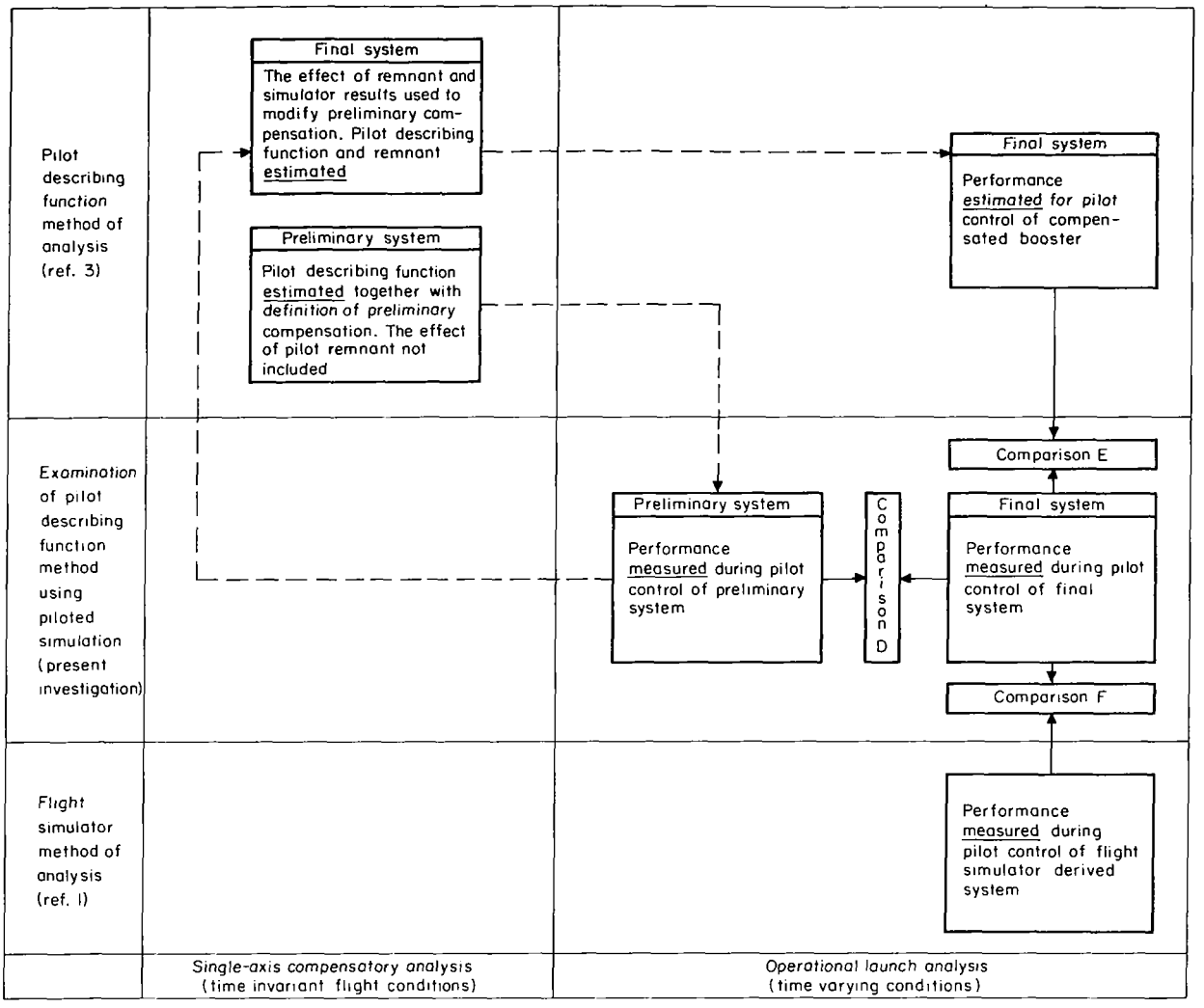

Figure 5.- Compensated booster.

method. The purpose of this comparison is to indicate the overall effectiveness of the pilot describing function method in formulating a final control system for a flexible vehicle.

RESULTS AND DISCUSSION

Uncompensated Booster

Single-axis compensatory analysis.- The first step of the pilot describing function study was a single-axis compensatory analysis. During this analysis, the pilot describing function, the attitude loop dynamics, the remnant, and the accelerations at the pilot station were estimated for the single-axis compensatory control of the booster dynamics. Standard servomechanism theory was applied to the problem.

Figure 6.- Saturn V simulation cab.

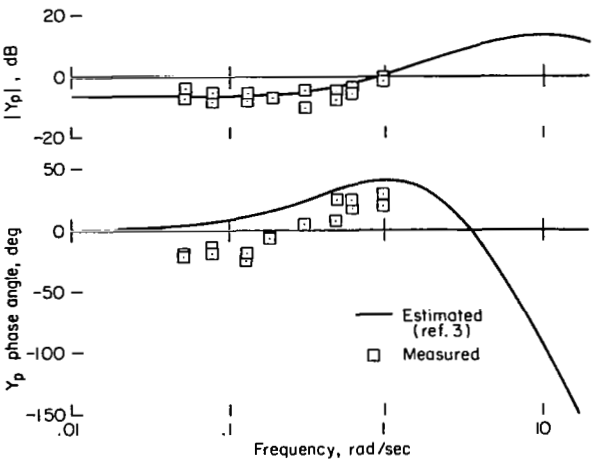

Figure 7.- Comparison A of figure 4: measured and estimated pilot describing function.

For the purpose of this analysis, the uncompensated system was programmed on a single-axis compensatory tracking task simulator. The cab used in the simulation is shown in figure 6. An attitude error was displayed on a cathode ray tube, the other displays were inactive. The system input was a random attitude signal, and the pilot's task was to null the attitude error. The simulation is further described in appendix B.

The quantities estimated in the pilot describing function study were measured (appendix B) using this simulation and the results are compared (comparison A of fig. 4). The measured and estimated pilot describing functions are compared in figure 7. The ordinate is given in radians of engine gimbal angle, β, per radian of attitude error, $\Delta\theta$. The symbols represent the measured describing function. The solid line represents the estimated describing function

$$Y_p = \frac{0.5(2j\omega + 1)e^{-0.2j\omega}}{\left(\frac{j\omega}{10}\right)^2 + 2(1)\left(\frac{j\omega}{10}\right) + 1}$$

from references 2 and 3. The amplitude ratios are in good agreement, but the measured phase angle is slightly lower than the estimated phase. It was noted in the pilot describing function study that additional phase lag should be included in the estimated describing function at the low frequencies to accurately represent the pilot. However, since the additional phase lag would not affect the system analysis (refs. 2 and 3), it was not included. On the basis of this comparison, the measured describing function agrees quite well with the estimated describing function.

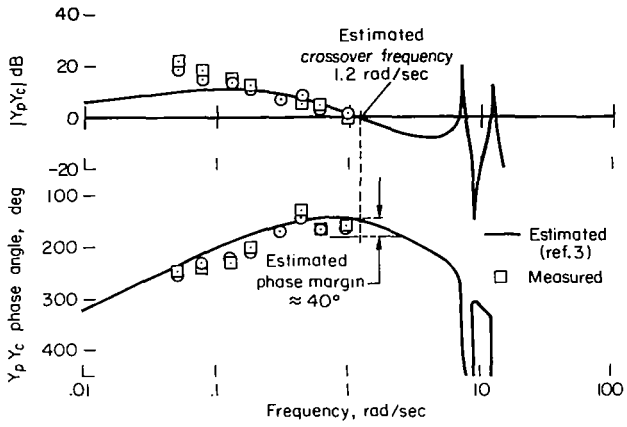

Figure 8.- Comparison A of figure 4: estimated and measured pilot-vehicle open-loop frequency response.

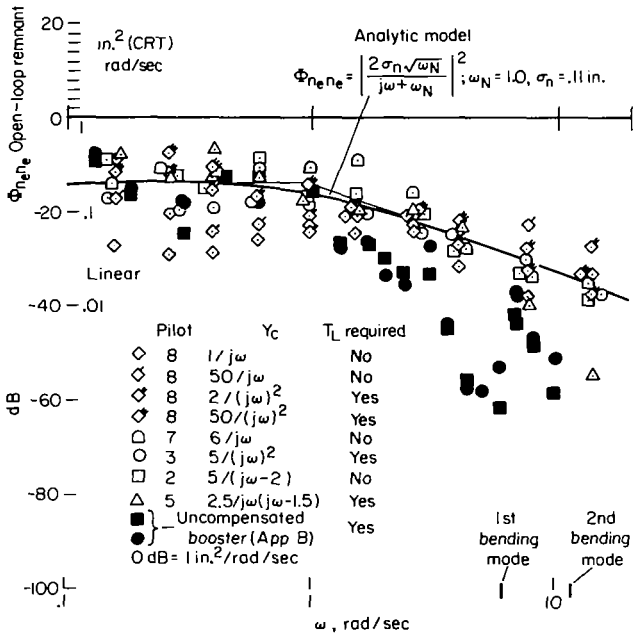

Figure 9.- Comparison A of figure 4: measured remnant data for uncompensated booster and data used in pilot describing function study (ref. 3).

The measured pilot-vehicle open-loop frequency response is compared with the estimated frequency response in figure 8. The solid line represents the estimated frequency response and the symbols represent the measured frequency response. The low-frequency characteristics are slightly different because of a difference between the equations of motion used in the pilot describing function study and those used in the present investigation. The difference is caused by the method used in making the equations time invariant. This is discussed further in appendix A. The frequency characteristics are similar, however, above 0.1 rad/sec. The measured crossover frequency (the frequency at which the amplitude ratio is 1) and the phase margin were approximately 1.0 rad/sec and 30°, respectively. The estimated crossover frequency and phase margin were approximately 1.2 rad/sec and 40°, respectively. The agreement between the measured and estimated values is considered good.

The methods used, during the pilot describing function study, to define a remnant model were not as definitive as those used to define the describing function. However, certain remnant data were available (ref. 4) during the analysis. These data were used to define a rudimentary remnant model, $\Phi_{nn_e} = \left|2\sigma_n\sqrt{\omega_N}/(j\omega + \omega_N)\right|^2$; $\omega_N = 1.0$; $\sigma_n = 0.11$ in., where σ_n is the root mean square of the pilot remnant.[2]

The remnant measured in this study is compared in figure 9 with the data and remnant model used in the pilot describing function study. The open symbols represent the data considered in the pilot describing function study (ref. 3) and the solid symbols represent the data measured in the present evaluation. The remnant model is indicated by the solid line. There is a

[2]The data presented here are correct, there was a factor of 2 error in the data and model presented in reference 3.

significant difference in the power between the remnant model and the remnant measured during the present study in the frequency range of the first and second bending modes. However, it should be noted that the data measured for the unstable dynamic element $2.5/j\omega(j\omega - 1.5)$ show better agreement with the booster data than the other recorded data. This is interesting since these dynamics are closest to the booster (see fig. 23 in appendix B).

The remnant model given by the solid line in figure 9 was used in the pilot describing function study to compute a normalized rms acceleration, $\sigma\gamma/\sigma_n$ = 30.9 m/sec^2-cm, at the pilot station caused by the elastic modes. Using the rms of the remnant model, σ_n = 0.11 in. = 0.2794 cm, the estimated rms acceleration would then be 8.633 m/sec^2 ≈ 0.9 g. The rms actually measured was ≈0.1 g. The difference between the measured and estimated rms is related to the difference between the measured and estimated remnant power at the elastic frequencies. A typical trace of the accelerations caused by the first bending mode, which was measured at the pilot station during a single-axis compensatory tracking task flight, is shown in figure 10. The magnitude varies between ±0.25 g.

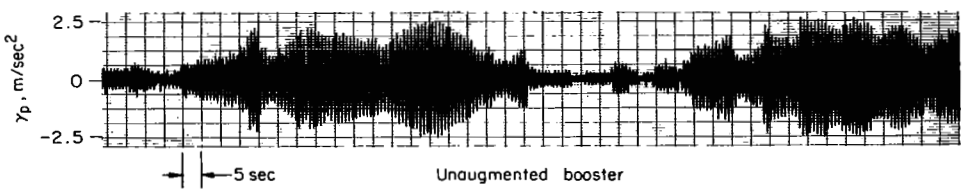

Figure 10.- Comparison A of figure 4: acceleration level at crew compartment due to first bending mode during single-axis compensatory tracking task (no pilot filter).

These comparisons (figs. 7-10) indicate that the linearized representation of the single-axis compensatory control of a flexible vehicle can be accomplished fairly well using existing pilot describing function estimation methods. However, some additional research appears necessary to define an accurate model of the pilot remnant.

Evaluation of operational launch analysis.- In the second step of the pilot describing function method, the results obtained in the single-axis compensatory analysis were used to indicate the system performance during an actual operational launch. These predictions were tentative in that they did not reflect the effects of pilot remnant. However, it was noted in the pilot describing function study that the estimated performance for this system would not correspond to the measured performance because the remnant was neglected and that some sort of pilot filtering would probably be required.

In the present investigation, the uncompensated booster without the pilot filter was simulated on a launch vehicle simulator and the performance

measured. The pilot display is illustrated in figure 11. Attitude and attitude error were displayed on the Flight Director Attitude Indicator (FDAI); vehicle acceleration, measured at a point near the vehicle instantaneous center of rotation, was displayed on the FDAI cross needles. Attitude rates were displayed on the rate meters. The pilot task was to follow a typical guidance profile, providing load relief during the encounter with a simulated wind disturbance.

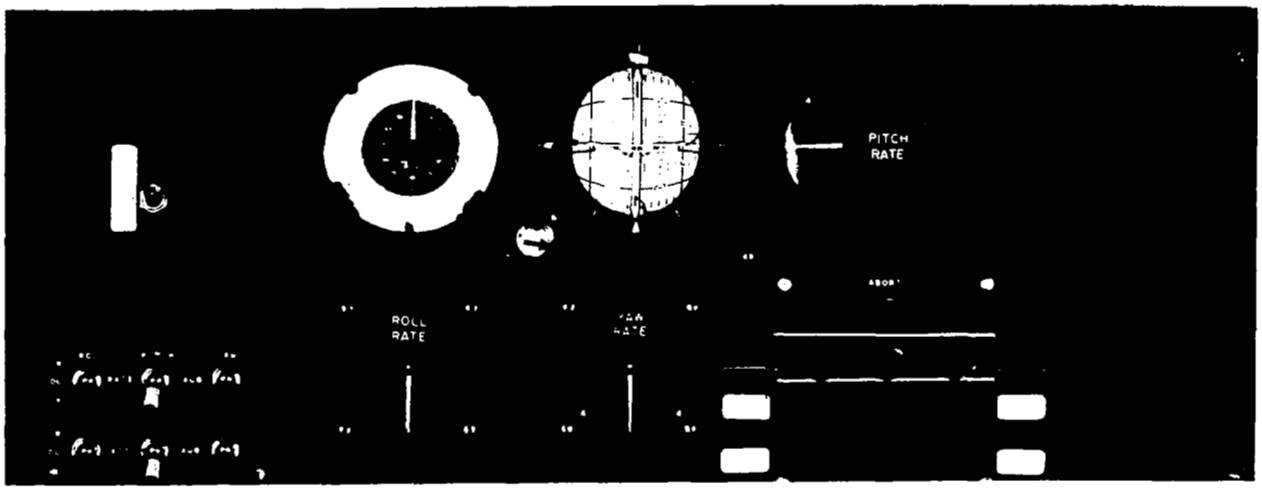

Figure 11.- Instrument panel used in launch simulator.

The measured performance for this system is compared (comparison B, fig. 4) with the estimated performance in figure 12. Performance data included are pilot rating, pilot comments, attitude guidance tracking, load

Performance	Estimated (ref. 2, 3) (Effect of remnant not included)	Measured (Launch vehicle simulator)
Pilot rating	5-8	10
Pilot comments	"Constant monitoring required to avoid overcontrol" "Tendency to emphasize control of high frequencies, which result in large-amplitude errors" "Best technique is to reduce frequency of control actions"	"Load relief impossible" "Attitude control very difficult" "Can't control the vehicle without causing severe excitations of the bending modes"
Attitude guidance tracking	"Poor, frequent exceedance of guidance tolerances"	"Excitation of bending modes prevented any accurate guidance tracking"
Load relief	Extremely difficult but possible	Impossible
Transverse accelerations at pilot station	None given	Severity of control prevented measurement

Figure 12.- Comparison B of figure 4: uncompensated booster (no pilot filter).

relief, and transverse accelerations at the pilot station. As expected, the measured performance is poorer with respect to all the criteria. The estimated performance indicates that the system would be difficult to control, but still flyable with a pilot rating of 5 to 8. The measured performance indicates that manual control is impossible and this is reflected in a pilot rating of 10. The primary cause of the poor measured performance is the severe excitation of the bending modes caused by the control actions of the pilot. This is clearly indicated by the pilot comments and accelerations measured at the pilot station. Since the trajectory guidance commands and the wind disturbance are of fairly low frequency, the excitation of the elastic modes cannot be explained by the describing function portion of the pilot model. It therefore seems reasonable to conclude that the difference between the estimated and measured performance for the system can be attributed to the effect of neglecting the pilot remnant in estimating the system performance.

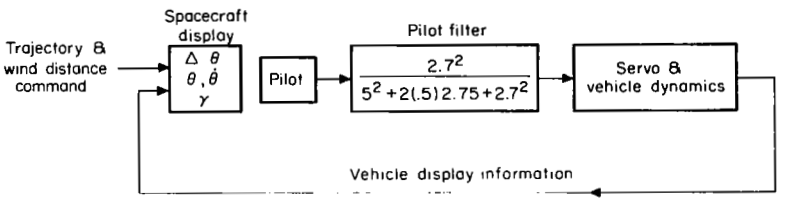

Figure 13.- Uncompensated booster - flight simulator derived system (ref. 1).

Performance	Flight simulator study, ref. 1. (Pilot filter)	Present simulation (No pilot filter)
Pilot rating	5-7	10
Pilot comments	"Difficult to control" "Constant attention required"	"Load relief impossible" "Attitude control near impossible" "Can't control vehicle without causing severe excitation of the bending modes"
Attitude guidance tracking	Fair	Excitation of bending modes prevented any accurate guidance tracking
Load relief	$M/M_D \approx .35 \rightarrow .7$	Impossible
Transverse accelerations at pilot station	$n_g = .03 - .05$	Severity of control prevented measurement

Figure 14.- Comparison C of figure 4: uncompensated booster performance - with and without pilot filter.

The uncompensated booster system derived using the flight simulator method (ref. 1) included a pilot filter and is illustrated in figure 13. The difference between this system and the one simulated in the present investigation is the filter located downstream of the pilot. The performance was presented for this system in reference 1. It is compared (comparison C, fig. 4) with the performance measured for the system without the pilot filter in figure 14. It is clear from this figure that the pilot filter improved the performance for the uncompensated booster. The pilot filter was designed to smooth the pilot control actions so as to reduce the excitation of the elastic modes without affecting the basic rigid-body dynamics (ref. 1). In terms of pilot describing function and remnant, this implies that the purpose of the pilot filter was to filter the pilot remnant.

It is interesting to compare the estimated performance for the system without the pilot filter (fig. 12) with the performance measured for the

system with the pilot filter (fig. 14). Since the estimated performance for the system without the pilot filter did not include the effect of pilot remnant, and since the purpose of the pilot filter was to reduce the effect of the pilot remnant without affecting the basic rigid-body dynamics, it seems reasonable that the estimated performance in figure 12 should compare reasonably well with the measured performance for the system with the pilot filter presented in figure 14. As is evident, the comparison between the two is good. The estimated pilot rating for the system without the pilot filter was 5 to 8, the measured pilot rating for the system with the pilot filter was 5 to 7.

Compensated Booster

The second problem considered during the pilot describing function study was the pilot control of a compensated booster. The purpose of this study was to formulate a compensation system of minimum complexity. As noted (fig. 5), this study proceeded in two phases. Initially, a preliminary compensation system was formulated to establish the basic stability augmentation for the system. The effect of pilot remnant was not considered in formulating this system. A final compensation was then formulated which did consider pilot remnant as well as other system integration factors (ref. 3) in the synthesis.

A single-axis compensatory analysis was conducted for both the preliminary and final systems in the pilot describing function study. This included an estimation of the pilot describing functions and remnant models used in the analysis (ref. 3). Unfortunately, these two systems were not simulated on a single-axis compensatory tracking task simulator in the present investigation and this portion of the pilot describing function method cannot be evaluated. The two systems were, however, simulated in a fixed-base launch vehicle simulator using the conventional operational pilot displays illustrated in figure 11.

The preliminary system is illustrated in figure 15. It is composed of two pilot control loops, attitude and load relief, and an inner loop that provides the basic vehicle compensation. The measured performance of this

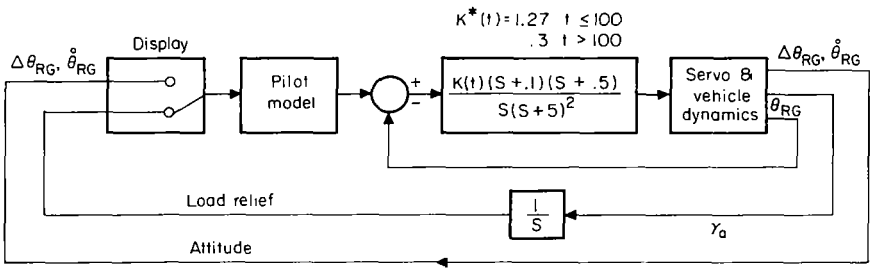

Figure 15.- Preliminary compensated booster (refs. 2, 3).

Performance	Measured (Launch vehicle simulator)
Pilot rating	5-7
Pilot comments	"Difficult to interpret displays during the load relief task" "Little feedback to pilot on the elastic dynamics" (fixed-base simulation) "Acceleration display useless, would hate to use in moving-base simulation"
Attitude tracking	Good
Load relief	$M/M_D \approx 1$
Transverse accelerations at pilot station	$n_g \approx .1 - .25$ g

Figure 16.- Measured performance for preliminary compensation system.

system is shown in figure 16. The system is satisfactory in attitude tracking, but not in pilot rating, load relief, and transverse accelerations at the pilot station. The main reason for the poor performance is an excessive excitation of the elastic modes caused by the pilot control actions. Since this was only a preliminary system, the performance was not estimated.

The performance measured for the preliminary system (fig. 16) was then used in the describing function study to aid in the establishment of a final integrated manual control system (ref. 3). The final system is illustrated in figure 17. The main difference between this system and the preliminary system is the

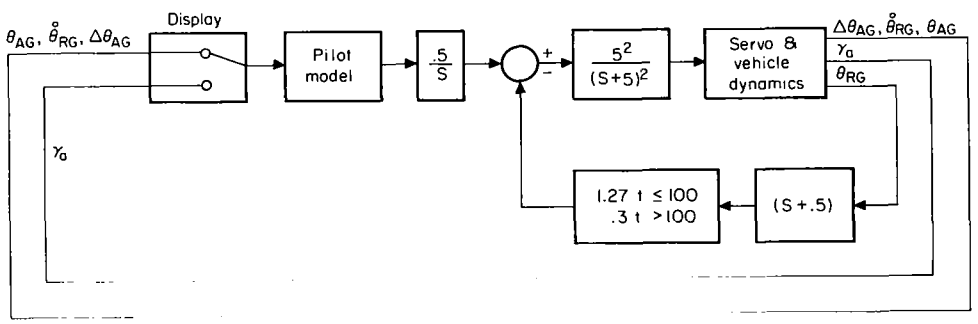

Figure 17.- Final compensated booster system.

placement of the (s + 0.5) lead in the feedback path of the inner loop and the placement of the integration term, 1/s, just downstream of the pilot (ref. 3). The (s + 0.1)/s term in the forward loop has also been eliminated. The primary purpose of these changes was to filter the high-frequency pilot output while retaining good attitude tracking and load relief control.

This system was flown on a piloted launch vehicle simulator and the performance measured. In contrast to the preliminary system, the final system provided an extremely smooth control system. The pilot control actions were effectively filtered, preventing the excessive excitation of the bending modes characteristic of the preliminary system. The performance for these two

systems is compared (comparison D, fig. 5) in figure 18. The performance for the final system is considerably improved over the performance measured for the preliminary system. The remaining adverse pilot comments were due to the gain change at $t = 100$ sec. Remnant was not used in defining the preliminary system, but was a primary factor in defining the final system (ref. 3). The above discussion clearly indicates the importance of remnant in the synthesis of a compensation system for a flexible vehicle.

Performance	Preliminary system	Final system
Pilot rating	5-7	3-4
Pilot comments	"Difficult to interpret displays during the load relief task" "Little feedback to pilot on the elastic dynamics" "Acceleration display useless, would hate to use in moving-base simulation"	"Very smooth system" "Large gain change at t=100 sec requires compromise on load relief" "Requires a lot of concentration and full control to null attitude error before gain change at t=100 sec"
Attitude tracking	Good	Good
Load relief	$M/M_D \approx 1.0$	$M/M_D \approx .5-.6$
Transverse accelerations at pilot station	$n_g \approx .1-.25$ g	$n_g \approx .02$ g

Figure 18.- Comparison D of figure 5: measured performance for preliminary and final systems.

Performance	Estimated (ref. 3)	Measured (Launch vehicle simulator)
Pilot rating	2-4	3-4
Pilot comments	None given	"Very smooth system" "Large gain change at t=100 sec requires compromise on load relief" "Requires a lot of concentration and full control to null attitude error before gain change at t=100 sec"
Attitude tracking	Good	Good
Load relief	$M/M_D \approx .35$	$M/M_D \approx .5-.6$
Transverse accelerations at pilot station	Minor	$n_g \approx .02$ g

Figure 19.- Comparison E of figure 5: estimated and measured performance for final compensated booster system.

The measured performance for the final system is also compared in figure 19 (comparison E, fig. 5) with performance estimated in the pilot describing function study for the final system. This comparison should indicate how well the results of the single-axis compensatory analysis can be generalized to the operational task in the pilot describing function method. The estimated and measured performances are in satisfactory agreement with respect to all the criteria listed.

The overall effectiveness of the pilot describing function method can be illustrated by comparing the performance measured for the final system with the performance measured for the different compensation system which was formulated using the flight simulator method (ref. 1). The compensated booster control system formulated using the flight simulator method of analysis is illustrated in figure 20. The inner loop provides the basic vehicle compensation. Filter immediately downstream of the pilot smooths the pilot output so as not to excite the elastic modes.

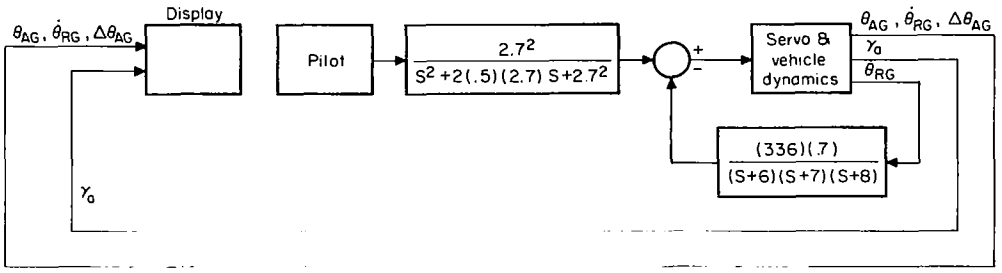

Figure 20.- Compensated booster - flight simulator system (ref. 1).

The measured performance for this system is compared (comparison F, fig. 5) with the measured performance for the final system formulated using the pilot describing function method in figure 21. Although the two systems are different in structure, the measured performance is very similar. The pilot rating of 3 to 4 was the same for the two systems. The system derived

Performance	Flight simulator derived system (ref. 1)	Pilot describing function derived system (ref. 3)
Pilot rating	3-4	3-4
Pilot comments	"Requires continuous concentration" "Generally pleasant"	"Very smooth system" "Large gain change at t = 100 sec requires compromise on load control" "Requires a lot of concentration and full control to null attitude error before gain change at t = 100 sec"
Attitude tracking	Good	Good
Load relief	$M/M_D \approx .4-.5$	$M/M_D \approx .5-.6$
Transverse accelerations at pilot station	$n_g \sim .03-.07$	$n_g \approx .02\,g$

Figure 21.- Comparison F of figure 5: measured performance for flight simulator derived and pilot describing function derived compensated booster systems.

using the pilot describing function method was slightly smoother than the simulator derived system. This is indicated by the pilot comments and transverse accelerations measured at the pilot station. The simulator derived system, however, provides some improvement in load relief. Based on these performance measures, both systems provide good manual control systems, and it can be concluded that the describing function method can provide a good estimate for a booster compensation system when all the dominant factors are included in the analysis.

CONCLUDING REMARKS

The pilot describing function method was used to analyze the manual control of a flexible booster. Because the method requires a number of approximations, it should be used in conjunction with a flight simulator program. Based on the present evaluation, it is concluded that existing pilot describing function data can be used to adequately represent the single-axis compensatory control of a flexible vehicle. The effect of the pilot remnant in the analysis of the flexible vehicle is, however, of much greater importance than it is in the analysis of the manual control of rigid vehicles, and additional research does seem necessary to establish a more definitive representation of the pilot remnant.

Despite the apparent limitations of the describing function method, the comparisons made in the present investigation indicate that it can be used successfully to synthesize a manual control compensation system for a large flexible booster.

Ames Research Center
National Aeronautics and Space Administration
Moffett Field, Calif., 94035, Jan. 7, 1969
125-19-01-16-00-21

APPENDIX A

CONSTANT COEFFICIENT EQUATIONS OF MOTION

The equations of motion used to represent the booster in the pilot describing function study were the same set used in the simulator study except that the coefficients were maintained constant at the values corresponding to the maximum dynamic pressure portion of the flight profile. This provides a set of constant coefficient linearized equations which, to a first approximation, represents the vehicle dynamics at a particular instant in time. However, a slightly different set of equations is available. The primary difference in the two sets of equations is their description of the low-frequency dynamics.

To illustrate this, it is sufficient to consider the equations of motion for the two-degree-of-freedom rigid-body dynamics. The representative set of time-varying coefficient equations of motion as used in the flight simulator study (ref. 1) is given below:

$$\ddot{x} = -F_\alpha \alpha - F_\theta \theta - F_\beta \beta \tag{A1a}$$

$$\Delta\ddot{\theta} = M_\alpha \alpha - M_\beta \beta \tag{A1b}$$

$$\alpha = \Delta\theta + \frac{\dot{x}}{V}(57.3) \tag{A1c}$$

These equations are a perturbation set with respect to a reference frame moving along the nominal trajectory. The axis, x, lies in the boost plane perpendicular to the nominal flight path; $\Delta\theta$ represents the attitude error sensed by the inertial navigator (in degrees), α represents the aerodynamic angle of attack (in degrees), and β is the engine control deflection (in degrees). The terms F_α, F_θ, F_β, M_α, M_β, and $57.3/V$ are time-varying coefficients where V is the nominal vehicle velocity (in m/sec). The validity of representing the vehicle dynamics at a particular instant of flight by constant coefficients is clearly dependent on the rate at which the respective coefficients vary. Using this method, the following set of constant coefficient linear equations is obtained:

$$\ddot{x}_1 = -0.13\alpha - 0.36\Delta\theta - 0.30\beta \tag{A2a}$$

$$\Delta\ddot{\theta} = 0.141\alpha - 1.15\beta \tag{A2b}$$

$$\alpha = \Delta\theta + 0.118\dot{x} \tag{A2c}$$

During the first stage burn, however, the launch vehicle is constantly accelerating. If the α equation is differentiated before the coefficients are set constant, the velocity, V, can be treated as a variable. The equation for α becomes

$$\dot{\alpha} = \Delta\dot{\theta} + \frac{\ddot{x}}{V} 57.3 - 57.3 \frac{\dot{x}}{V}\frac{\dot{V}}{V} = \Delta\dot{\theta} + \frac{\ddot{x}}{V} 57.3 - (\alpha - \Delta\theta)\frac{\dot{V}}{V}$$

With the coefficients of this equation held constant at the maximum dynamic pressure values, the following set of equations represents the vehicle dynamics:

$$\ddot{x} = -0.13\alpha - 0.36\Delta\theta - 0.30\beta \tag{A3a}$$

$$\Delta\ddot{\theta} = 0.141\alpha - 1.15\beta \tag{A3b}$$

$$\dot{\alpha} = \Delta\dot{\theta} + 0.118\ddot{x} - (0.03086)(\alpha - \Delta\theta) \tag{A3c}$$

These two sets of equations are compared in terms of their frequency response and transfer functions in figure 22. It is seen that the frequency response for the second set of equations ((A3a) - (A3c)) has a much higher low-frequency gain than does the first set of equations. The first set of equations would suggest poor low-frequency response (refs. 2 and 3). The second set of equations, however, exhibits a higher gain in the low-frequency dynamics and does not indicate a poor low-frequency response. The latter is more consistent with actual pilot performance in a simulator using the time-varying vehicle dynamics (ref. 1) and therefore appears to be a better estimation of the time-varying set of differential equations.

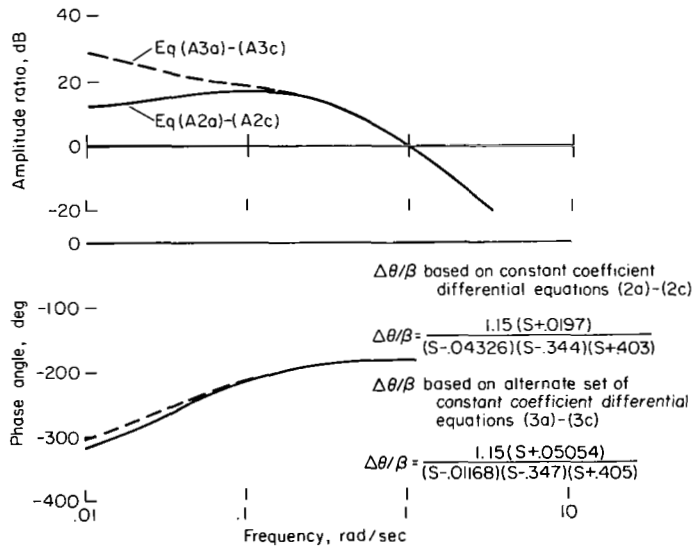

Figure 22.- Comparison of frequency response for two time-invariant representations of the booster dynamics.

APPENDIX B

QUASI-LINEAR PILOT MODEL MEASUREMENTS

Measurements were made of a pilot controlling the unaugmented launch vehicle dynamics without a pilot filter in a single-axis compensatory tracking task. For these tests, the launch vehicle dynamics were reduced to a set of time-invariant dynamics representative of the system 77 seconds into the flight. At this time, the vehicle is in the high dynamic pressure portion of the trajectory. The equations were reduced to a time-invariant set using the second method in appendix A, equations (A3a) to (A3c).

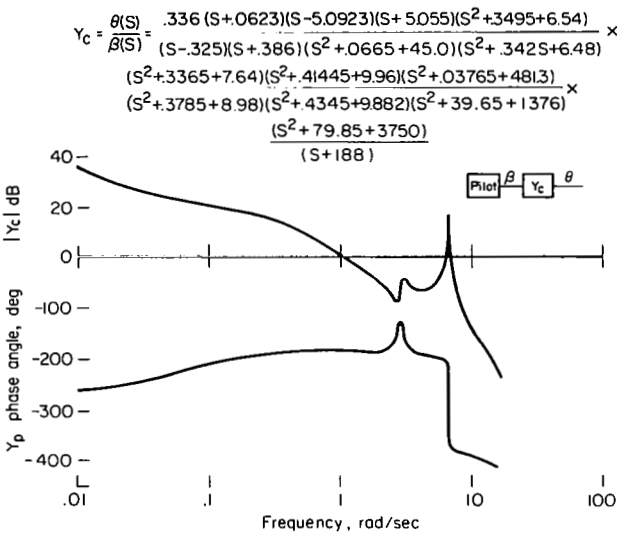

Figure 23.- Attitude to engine gimbal command angle frequency response.

An existing Saturn V launch vehicle simulation (ref. 12) was converted to the constant coefficient linearized approximation of the actual vehicle dynamics. The frequency response for the uncompensated booster attitude dynamics and the respective transfer function is shown in figure 23.

During these tests, the pilot was given a random-appearing attitude tracking task in the pitch plane. The attitude error was displayed to the pilot by a horizontal bar on the cathode ray tube. The input signal was prerecorded on an FM tape recorder.

The frequency range of the input signal used during the pilot describing function measurements was made compatible with the vehicle response requirements during a piloted launch. To understand how the response requirements on the vehicle were determined, it is necessary to review the pilot task during launch. The primary pilot task during a launch is to guide the vehicle through the first stage of flight and to reduce the structural loads on the vehicle by keeping the vehicle headed into the wind. The latter maneuver predominates as the vehicle penetrates the jet stream, and this maneuver establishes the fastest response requirements on the system. This response requirement can be represented in the continuous tracking task by adjusting the bandwidth of the input signal to be near the bandwidth of the Fourier transform of the wind disturbance. The physical significance of this technique is explained in references 3 and 13.

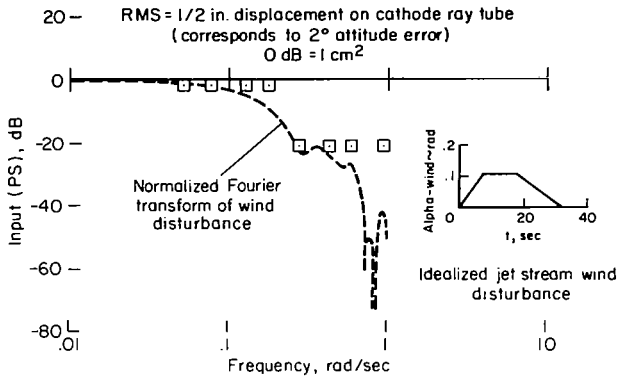

Figure 24.- Input power spectrum.

The spectrum of the input signal is compared with the Fourier transform of the wind disturbance in figure 24. The input signal was composed of eight sine waves, four primary and four secondary. The frequencies of the sine waves were adjusted so that each sine wave gave a prime number of cycles within a four-minute interval. The attitude tracking signal was therefore periodic with a fundamental period of four minutes. This low fundamental frequency in the command signal was not evident to the pilot and the resulting signal appeared to be random. The four primary frequencies of the random-appearing input signal had a bandwidth of 0.183 rad/sec. The secondary frequencies were reduced to one-tenth the amplitude of the primary frequencies and ranged in frequency from 0.204 to ≈1 rad/sec. This "augmented rectangular input spectrum" provides a command signal in the frequency range of booster task demands, less than 0.183 rad/sec, and still provides some energy at higher frequencies without affecting the low-frequency performance of the pilot (ref. 4). This type of input signal allows pilot model measurements at frequencies higher than the primary input signal bandwidth. The technique has been used successfully before and is described more completely in reference 4.

The command input, the error signal, the pilot output, and the vehicle output (fig. 1) were recorded on FM tape. Data were recorded in four-minute intervals. Since all sine waves composing the input exhibited an integral number of cycles in a four-minute period, a zero mean was assured. The signals were analyzed for their power and cross-power content and the transfer function of the pilot was estimated using standard relations for power density spectra in linear systems. These techniques are covered thoroughly in references 14, 15, and 16. The actual relations used to estimate the pilot model and the total open-loop system representation are given below.

$$Y_p(j\omega) = \frac{\Phi_{ic}(j\omega)/\Phi_{ii}(j\omega)}{\Phi_{ie}(j\omega)/\Phi_{ii}(j\omega)} \tag{B1}$$

$$Y_pY_c(j\omega) = \frac{\Phi_{im}(j\omega)/\Phi_{ii}(j\omega)}{\Phi_{ie}(j\omega)/\Phi_{ii}(j\omega)} \tag{B2}$$

$$\rho^2(j\omega) = |\Phi_{ic}(j\omega)|^2/\Phi_{ii}(j\omega)\Phi_{cc}(j\omega) \tag{B3}$$

$$\Phi_{nn}(j\omega) = [1 - \rho^2(j\omega)]\Phi_{cc}(j\omega) \tag{B4}$$

$$\Phi_{n_e n_e}(j\omega) = \left|\frac{1 + Y_p Y_c}{Y_p}\right|^2 \Phi_{nn}(j\omega) \tag{B5}$$

where

$c(t)$	pilot output
$e(t)$	error signal (displayed to the pilot)
$i(t)$	command signal
$m(t)$	system output
$n(t)$	that portion of the pilot output not linearly correlated with the command signal
$n_e(t)$	signal that, if injected at the pilot's eye, would cause the signal $n(t)$ in the pilot output considering an otherwise completely linear system
$\Phi_{xy}(j\omega)$	cross power between $x(t)$ and $y(t)$

REFERENCES

1. Hardy, Gordon H.; West, James V.; and Gunderson, Robert W.: Evaluation of Pilot's Ability to Stabilize a Flexible Launch Vehicle During First-Stage Boost. NASA TN D-2807, 1965.

2. Jex, H. R.; Teper, G. L.; McRuer, D. T.; and Johnson, W. A.: A Study of Piloted Saturn V Booster Problems Using Analytical Pilot Models and Unified Servo-Analysis Techniques. Tech. Rep. 144-1, Systems Technology, Inc., April 1965.

3. Jex, H. R.; Teper, G. L.; McRuer, D. T.; and Johnson, W. A.: A Study of Fully-Manual and Augmented-Manual Control Systems for the Saturn V Booster Using Analytical Pilot Models. NASA CR-1079, 1968.

4. McRuer, D. T.; Graham, D.; Krendal, Ezra; Reisener, William, Jr.: Human Pilot Dynamics in Compensatory Systems. Theory, Models, and Experiments with Controlled Element and Forcing Function Variations. Rep. AFFDL-TR-65-15,USAF Flight Dynamics Laboratory, July 1965.

5. Stapleford, R. L.; Johnston, D. E.; Teper, G. L.; and Weir, D. H.: Development of Satisfactory Lateral-Directional Handling Qualities in the Landing Approach. NASA CR-239, 1965; also see J. Aircraft, vol. 3, no. 3, 1966, pp. 201-7.

6. Cromwell, C. H.; and Ashkenas, I. L.: A Systems Analysis of Longitudinal Piloted Control in Carrier Approach. Final Report, TR-124-1, Systems Technology, Inc., June 1962.

7. Muckler, F. A.; and Obermayer, R. W.: The Use of Man in Booster Guidance and Control. NASA CR-81, 1964.

8. Muckler, F. A.; and Hookway, R. O.; and Burke, H. H.: Manned Control of Large Space Boosters. Trans. Seventh Symposium on Ballistic Missiles and Space Tech., Vol. II, Aug. 1962, pp. 149-188.

9. Kilpatric, Philip S.: Bending Mode Acceleration Influence on Pilot Control of Flexible Booster Dynamics. T-65-2, Massachusetts Institute of Technology, Sept. 1965.

10. Stapleford, R. L.; and Craig, S. J.: Measurement of Pilot Describing Functions in Single-Controller Multiloop Tasks. TR 167-1, Systems Technology, Inc., Aug. 1967.

11. Cooper, George E.: The Use of Piloted Flight Simulators in Take-off and Landing Research. Presented at the Take-Off and Landing Specialists Meeting, Flight Mechanics Panel, AGARD, Paris, France, January 14-18, 1963.

12. Hardy, Gordon H.; Kurkowski, Richard L.; and Ritter, Glen D.: The Reliability Contribution of the Pilot to a Large Launch Vehicle Control System. AIAA Paper 67-554, 1967.

13. Halfman, Robert L.: Dynamics. Vol. 2, Addison-Wesley Publishing Co., Reading, Mass., 1962.

14. Hall, Ian A. M.: Effects of Controlled Element on the Human Pilot. WADC TR-57-509, Princeton University, August 1958.

15. Newton, G. C.; Gould, L. A.; and Kaiser, J. F.: Analytical Design of Linear Feedback Controls. John Wiley and Sons, Inc., New York, 1957.

16. Graham, D.; and McRuer, Duane: Analysis of Nonlinear Control Systems. John Wiley and Sons, Inc., New York, 1961.

NASA-Langley, 1969 —— 21 A-2825